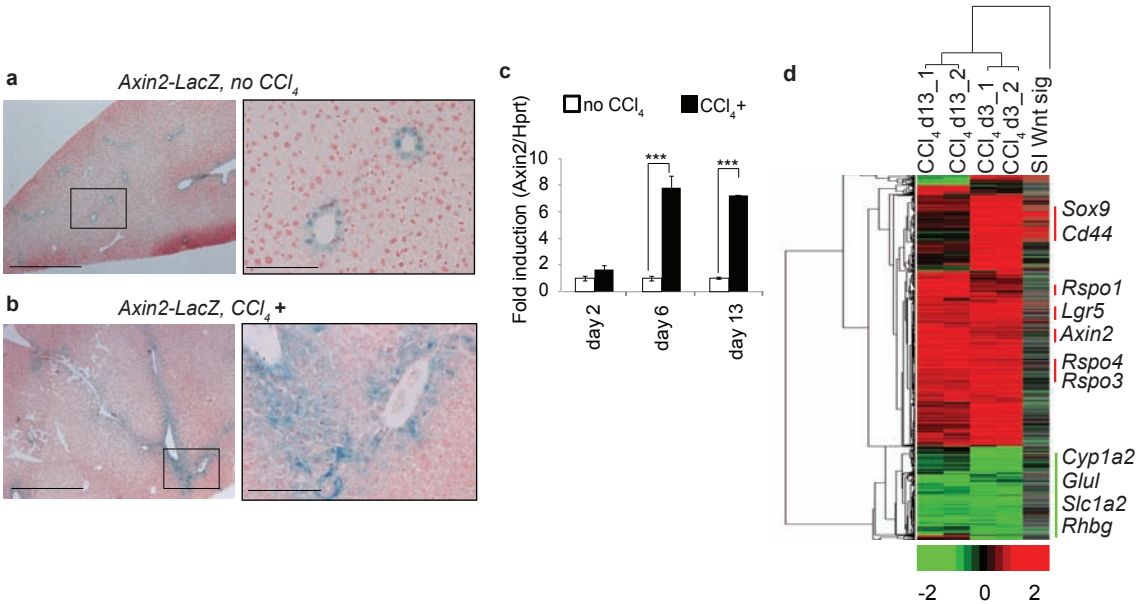

Supplementary Figure 1. Wnt induction in the liver upon CCl_4 damage

a-b, *Axin2-LacZ* mice were injected (IP) with corn oil (no CCl_4, n=6) or with a single dose of CCl_4 in corn oil (CCl_4 +, n=6). Six days later, mice were sacrificed and livers collected for β-gal staining. **a**, Healthy mouse liver shows *Axin2-LacZ* expression restricted to perivenous hepatocytes. **b**, *Axin2-LacZ* expression extends towards periportal areas upon CCl_4-treatment. Scale bars, 500 μm (left panels) and 100 μm (right panels). **c**, qPCR analysis of *Axin2* mRNA in adult liver upon CCl_4 administration. Results are represented as mean ± SEM of at least 3 independent experiments. *Hprt* was used to normalize for expression levels. Non-parametric Mann-Whitney test was used. ***$p<0.0001$. **d**, Hierarchical clustering analysis showing genes differentially expressed at days 3 or 13 after treatment relative to non-damaged liver. Alignment of the reported small intestinal wnt target signature (ref.8) to the liver genes shows that many of the intestinal Wnt target genes are also upregulated after damage (red bar). Known perivenous wnt target genes (ref. 14) are downregulated (green bar). Representative genes are indicated. Scale bar indicates gene expression in log2 ratio. Red colour, upregulated; green, downregulated; grey, not expressed.

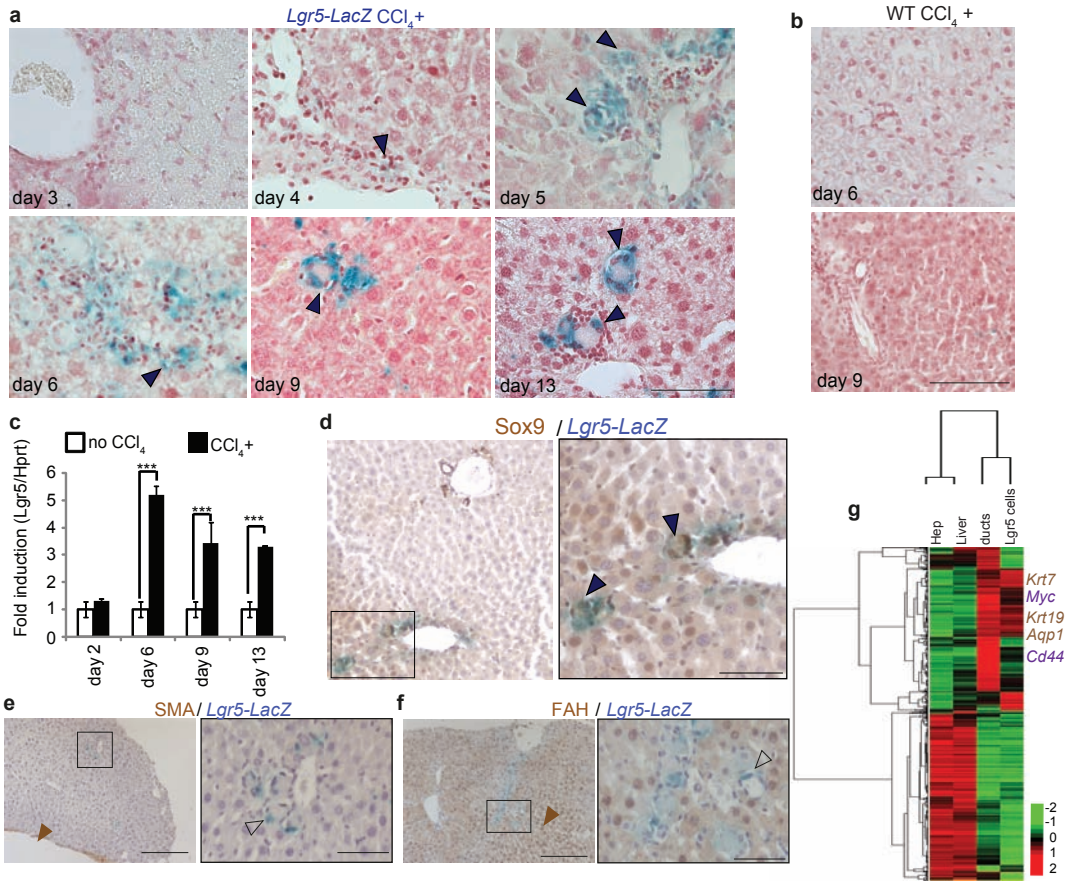

Supplementary Figure 2. Lgr5-LacZ expression upon liver damage

a-f, *Lgr5-LacZ* mice (n=10) and WT littermate controls (n=5) received a single IP injection of CCl_4. Livers were harvested at the indicated days and processed for RNA or b-galactosidase staining. **a**, X-gal staining was exclusively detected in duct-like small cells (arrowheads) in the *Lgr5-LacZ* mice. **b**, No staining was observed in WT control littermates. **c**, qPCR analysis of Lgr5 mRNA in adult liver upon CCl_4 administration. Results are represented as mean ± SEM of at least 3 independent experiments. *Hprt* was used to normalize for differences in expression levels.***, p<0.0001. **d**, *Lgr5-LacZ* positive cells co-stained with the ductal progenitor marker Sox9 (arrowheads). **e-f**, *Lgr5-LacZ*+ cells did not co-stain with the stellate cell marker smooth muscle actin (**e**, SMA, empty arrowheads) or with the hepatocyte marker FAH (**f**, empty arrowheads). Both markers were positive in the surrounding connective tissue (**e**, SMA, brown arrowhead) or surrounding hepatocytes (**f**, FAH, brown arrowhead). Scale bars, 100 µm (**a-b**), 0,5 mm (**e-f,** left panel), 50µm (**d-f,** right panel). **g**, *Lgr5*+ cells were sorted from *Lgr5-LacZ* mice treated with CCl_4 as described in Fig. 2. Hierarchical clustering analysis of the average of biological replicates of *Lgr5-LacZ*+ sorted cells, MIC1-1C3+ sorted ductal cells, liver tissue and hepatocytes (Hep). Lgr5+ cells clustered together with ductal cells whereas they did not resemble to hepatocytes. Representative genes are indicated (brown, ductal marker; purple, wnt target and stem cell marker). Scale bar, gene expression in log2 ratio. Red colour, upregulated; green, downregulated.

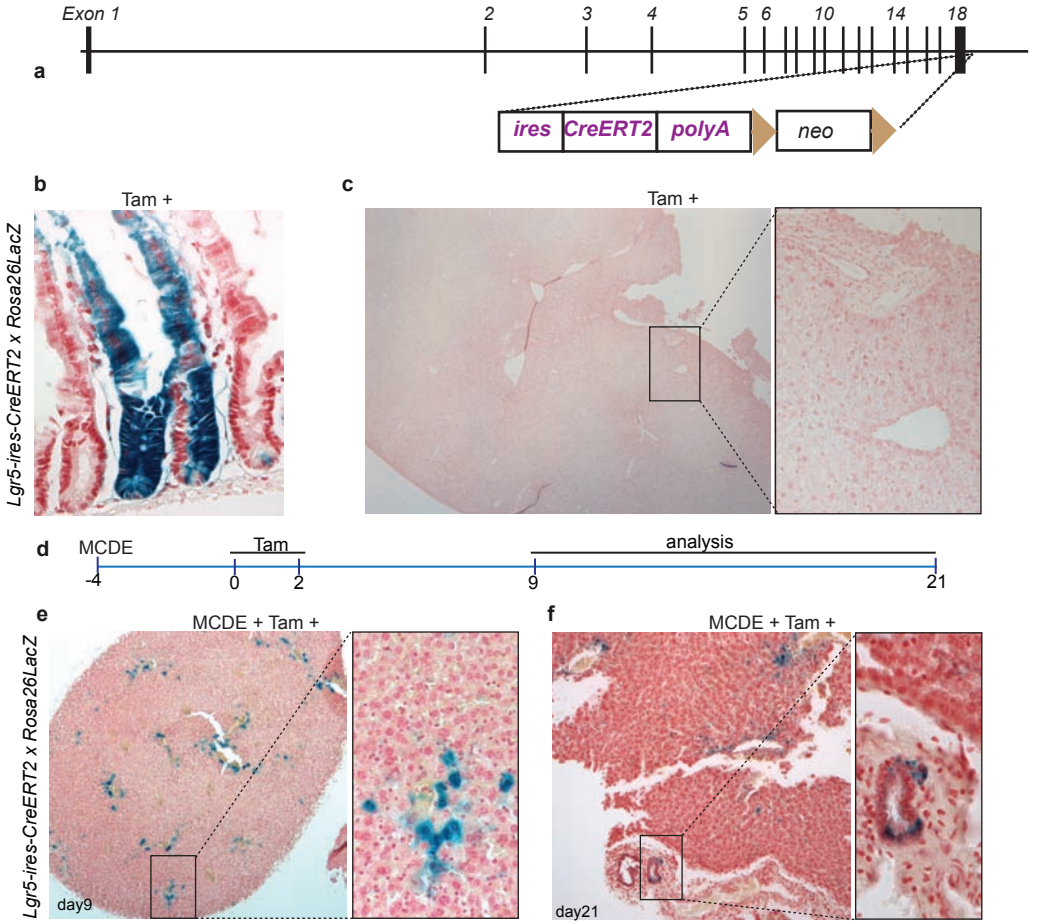

Supplementary Figure 3. *Lgr5-ires-CreERT2* tracing

a-c, Validation of novel Lgr5 allele. *Lgr5-ires-CreERT2* mice were crossed with the *Rosa26-LacZ Cre* reporter line and 8-12 weeks after birth mice were injected with tamoxifen. Nine days later, mice were sacrificed and small intestine (**b**) and liver (**c**) were collected for X-gal staining analysis. **a**, Scheme of the *Lgr5-ires-CreERT2* allele indicating the site of insertion of the *ires-CreERT2* cassette in the *Lgr5* locus. **b**, Note the blue ribbons on small intestine at day 9 after induction, indicative of stem cell tracing events. **c**, No tracing events were detected under physiological conditions in the liver of *Lgr5-ires-CreERT2 x Rosa26-LacZ* mice 45 days after tamoxifen induction. Magnification: 5x (left panel), 20x (right). **d-f**, *Lgr5-ires-CreERT2 x Rosa26-LacZ* mice (8-12 week-old) were fed with MCDE (methionine choline-deficient ethionine supplemented diet) (n=4) to induce liver damage. CreERT2 activity was induced by 2 doses of tamoxifen (3mg/mouse) 4 and 6 days later. **d**, scheme indicates the protocol used. **e,** Representative images of X-gal positive hepatocytes within the liver parenchyma of an MCDE treated mouse 9 days after tamoxifen induction. Magnification 5x (left panel), 20x (right panel). **f**, X-gal positive ducts within the liver tissue of an MCDE treated mouse 21 days after tamoxifen induction. Magnification, 10x (left panel), 40x (right panel).

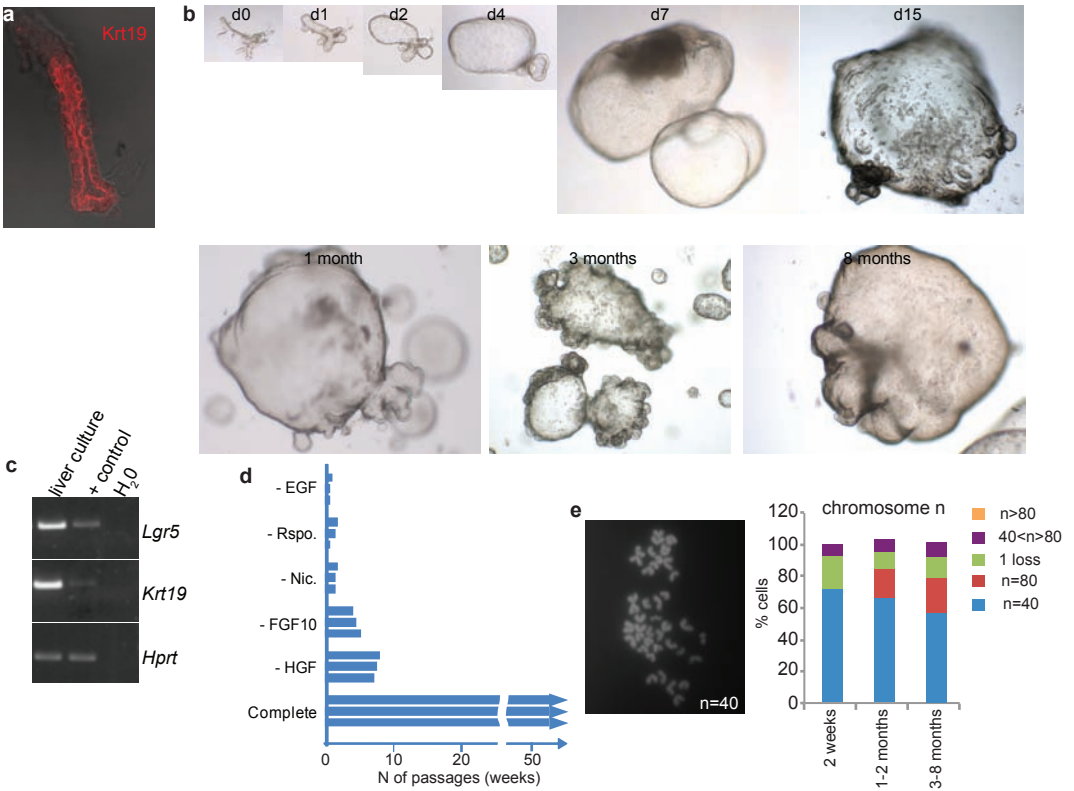

Supplementary Figure 4. Liver organoids are genetically stable and self-renew long term when cultured under defined Expansion Medium

a-e, Biliary duct fragments were isolated and cultured for more than 8 months as described in the material and methods. **a**, Krt19 staining in an isolated biliary duct fragment. **b**, Representative images of biliary ducts growing into liver organoids at the indicated time points. Original magnifications: 10x (day 0, 1, 2, 4) and 4x (day 7 onwards). **c**, *Lgr5* and *Krt19* gene expression by RT-PCR on liver organoids. *Hprt* gene was used to normalize for differences in RNA input. **d**, Liver-derived organoids were cultured as described in Methods ('complete'), or in the absence of individual components, as indicated. Each horizontal bar represents an independent experiment. Each experiment was done in duplicate. Nic, nicotinamide. Rspo, rspondin. **e**, Chromosomal numbers were counted in liver organoids after 2 weeks, 1-2 months and >3 months (3-8 months) in culture. Two independent cultures were used (1 derived from duct fragments and the other clonal). ~100 spreads were counted in total. Representative karyotype of an 8 month-old liver culture with n=40 chromosomal counts. Graph plots the % of cells with chromosomal counts n=40, n=80, 1 loss (n=39 or n=79) and aneuploidy 40<n>80 and n>80. Aneuploidy was ~20% at all time points. No cells with n> 80 were observed at any time point, indicating that the cells are genetically stable.

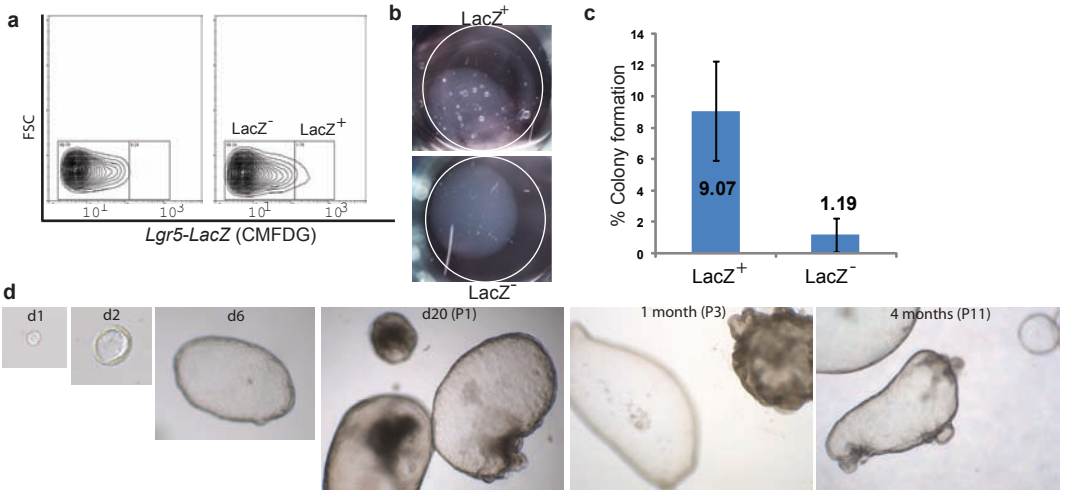

e **Colony formation efficiency of *Lgr5* liver secondary cultures**

	Experiment I		Experiment II		Experiment III	
	Lgr5 positive	Lgr5 negative	Lgr5 positive	Lgr5 negative	Lgr5 positive	Lgr5 negative
n cells input (d0)	100	100	125	1620	60	30
n organoids (d10)	14	0	4	4	6	1
% colony formation	14	0	3.2	0.25	10	3.33

Colony formation efficiency of *Lgr5* cultures derived from liver tissue after CCl_4 treatment

	Experiment I		Experiment II		Experiment III	
	Lgr5 positive	Lgr5 negative	Lgr5 positive	Lgr5 negative	Lgr5 positive	Lgr5 negative
n cells input (d0)	1000	3000	200	400	400	3000
n organoids (d14)	19	14	5	3	11	23
% colony formation	1.9	0.47	2.5	0.75	2.75	0.77

Supplementary Figure 5. Clonal expansion of single Lgr5 cells from *Lgr5-LacZ* liver organoid cultures
a, FACS plot of *Lgr5-LacZ* hepatic organoids stained for LacZ with Detectagene Green CMFDG. Cells were FACS-sorted as described in Fig.2. FSC: forward scatter. **b**, Representative images showing 100 sorted Lgr5-LacZ+ cells growing into liver organoids 10 days after sorting. **c**, Graph showing the % of colony formation. **d**, Representative serial DIC images showing the outgrowth of a single Lgr5-LacZ+ cell. Original magnifications: 40x (days 1-2), 20x (day 4), 10x (day 6), 4x (day 20 onwards). P, passage. **e**, Table giving the numbers used to calculate the % colony formation for both, secondary cultures (top table) and cultures started from *Lgr5-LacZ* mice treated with CCl_4 (bottom table).

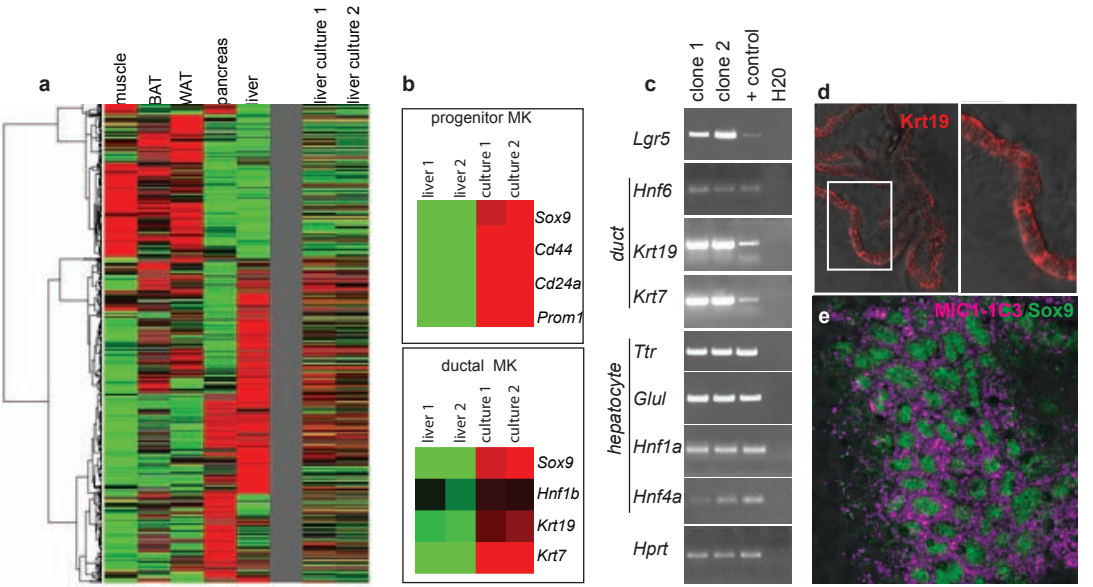

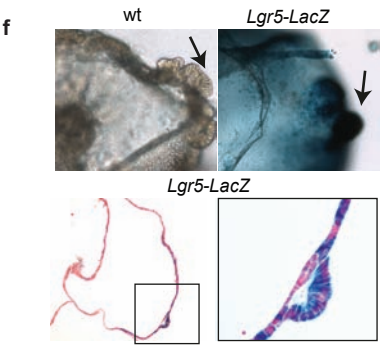

Supplementary Figure 6. Gene expression profile and characterization of liver organoids in Expansion Medium

a, Expression profile comparison of liver organoids against five different tissues (BAT, brown adipose tissues; WAT, white adipose tissues; muscle; liver and pancreas). Hierarchical clustering of genes differentially expressed among five different tissues with > 4-fold changes after mean-centering, and the comparison of the corresponding expression patterns in liver organoids. **b**, Heat-map shows representative progenitor and biliary duct genes strongly expressed in clonal Lgr5 derived liver cultures compared to adult liver tissues. **c**, RT-PCR gene expression analysis of selected hepatocyte or biliary duct markers on 1-2 month-old clonal cultures. Two independent clones were analyzed. + control, small intestine (*Lgr5*) and liver (duct and hepatocyte genes). *Hprt* was used to normalize for differences in RNA input. **d**, confocal image of liver organoids stained for Krt19. Note that the ductal marker Krt19 is marking single layered epithelium within the oganoid. **e**, Sox9 (green) and ductal marker MIC1-1C3 (magenta) immunofluorescent staining in liver organoids. Note that many cells are positive for both markers. **f**, DIC image of wild type control (wt, top left) or *Lgr5-LacZ* liver organoids (top right) stained for X-gal. Arrows, budding structures. Magnification, 20x. Lower panels; section from an X-gal stained *Lgr5-LacZ* liver organoid showing LacZ+ expression restricted to the budding, single layered compartment, of the organoid. Magnification, 10x (left) and 40x (right).

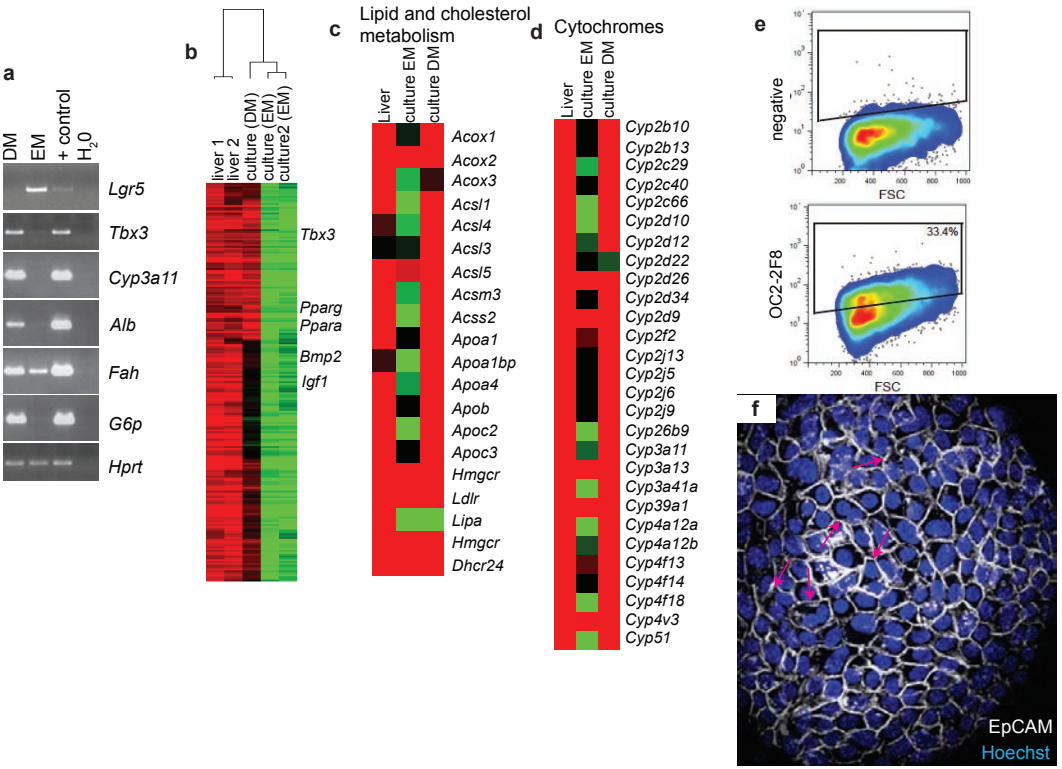

Supplementary Figure 7. Gene expression profile of liver organoids in DM

a-f, Cultures were maintained under expansion medium (EM) or transferred to differentiation medium (DM) for 9-14 days. Then, cultures were collected and processed for gene expression analysis or fixed and stained as described in Methods. **a**, RT-PCR gene expression analysis of *Lgr5* and liver-specific genes *Tbx3, Cyp3a11, Alb, Fah* and *G6p.* Experiments were performed with 2 independent clonal cultures. Representative images are shown. *Hprt* was used to normalize for differences in expression levels. +, liver tissue or small intestine (*Lgr5*). **b-d**, Microarray and hierarchical clustering analysis evaluates genes differentially expressed between cultures maintained in EM, DM or liver tissue. **b**, Heat-map of the cluster of 215 transcripts upregulated (>4 fold) both in adult liver tissues and under DM compared to EM. Representative induced genes are listed. **c**, Heat-map showing significantly upregulated lipid and cholesterol metabolic genes after DM (>2-fold, $p<0.05$ after mean centering). **d**, Heat-map showing significantly upregulated cytochrome genes upon differentiation (>2-fold, $p<0.05$). Red, upregulated; green, downregulated; black, no change. **e**, Clonal Lgr5-derived cultures maintained under DM for 9 days were labeled with the hepatocyte surface marker OC2-2F8 and analyzed by flow cytometry. OC2-2F8 labeling was detected by APC-conjugated anti-rat Ig; dead cells were excluded by PI labeling. **f**, Bi-nucleated cells (arrows) appear in liver organoids after 14 days of DM. EpCAM cell surface marker was used to visualize cell-cell border while nuclei where stained with Hoechst.

.

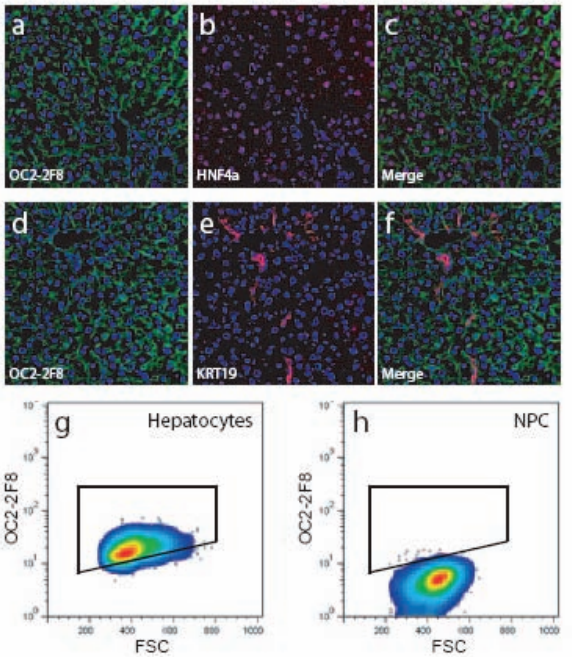

Supplementary Figure 8. Antibody OC2-2F8 recognizes mature hepatocytes

a-f, Labeling of acetone-preserved normal mouse liver by OC2-2F8 was detected by Cy3-conjugated anti-rat Ig. HNF4a co-staining (**a-c**) confirms that OC2-2F8 antibody stains hepatocytes, whereas Krt19+ ductal cells are negative for OC2-2F8 (**d-f**). Original magnification: 100x. **g-h**, Flow cytometry analysis of Liver isolated hepatocytes (**g**) or Non Parenchymal Cells (**h**) after OC2-2F8 and APC-conjugated anti-rat Ig labeling. Hepatocyte and NPC populations were obtained by differential centrifugation and size/granularity gating.

a

Experimental groups	n mice group	donor cells	n mice analyzed FAH	pos. FAH staining	PCR confirmation
Group A	8	Lgr5-GFP organoids (clone I)	5 #	2	pos (2/2)
Group B	6	Lgr5-LacZ organoids (clone II)	5 #	1	pos (1/1)
Group C	5	Lgr5-LacZ organoids (clone III)	5 ^	2	pos (2/2)
Group D	3	HEPATOCYTES (+control)	3	3	-
Group E	4	No cells (-control)	2 #	0	-

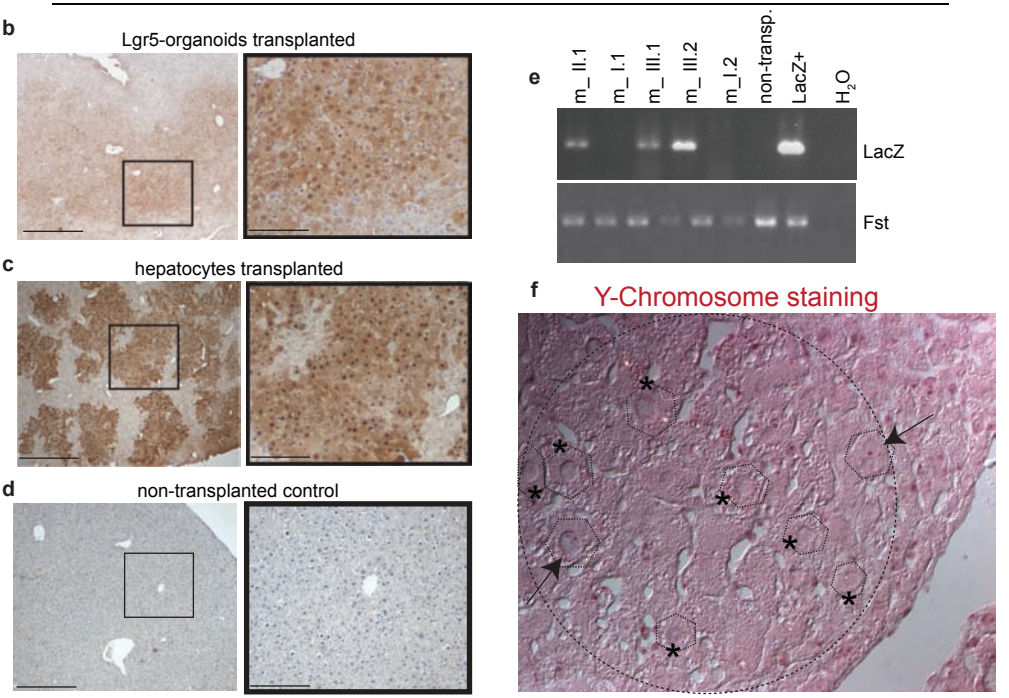

Supplementary Figure 9. Analysis and validation of FAH+ clones and transplantation efficiency

a, Table summarizing the transplantation protocol and engraftment results. # Some mice died in the course of the experiment and tissues could not be collected nor analyzed for the presence of engraftment. ^For this group, 1 mouse was sacrificed at an early time point (day 15) for engraftment analysis purposes. This mouse was removed from the study in the subsequent survival analysis. **b**, FAH+ area within the liver parenchyma (section from a mouse transplanted with clone I). Scale bar, 200um (left) and 100 um (right). **c**, FAH+ area within the liver parenchyma (section from a mouse transplanted with hepatocytes as positive control). Scale bar, 200um (left) and 100 um (right). **d**, Non-transplanted *Fah-/-* mouse underwent similar NTBC withdrawal protocol. No FAH staining is detected. Scale bar, 200um (left) and 100 um (right). **e**, Detection of *LacZ* gene from donor cells by genomic PCR analysis. DNA was isolated from FAH+ areas from paraffin sections. *Fst,* Follistatin, control for genomic DNA quality. non-transp., liver tissue from a paraffin section of a non-transplanted control. **f**, Y-chromosome staining on a serial section of the grafted area displayed in Figure 4 (circle). Negative Y-chromosome staining indicates the absence of fusion between female donor cells and recipient male mouse hepatocytes (n=3). *, Y chromosome-negative nuclei in the grafted area. Arrows, Y chromosome+ nuclei in the boundary between the grafted and non-grafted tissue. Magnification: 40x. DIC microscopy was used to better visualize nuclei.